sensors

MDPI

Article

Effect of MgO Underlying Layer on the Growth of GaO_x Tunnel Barrier in Epitaxial Fe/GaO_x/(MgO)/Fe Magnetic Tunnel Junction Structure

Sai Krishna Narayananellore [1], Naoki Doko [1,2], Norihiro Matsuo [1,2], Hidekazu Saito [1,*] and Shinji Yuasa [1]

[1] National Institute of Advanced Industrial Science and Technology (AIST), Spintronics Research Center, Umezono 1-1-1, Central 2, Tsukuba, Ibaraki 305-8568, Japan; narayananellore-sk@aist.go.jp (S.K.N.); dokou.n@aist.go.jp. (N.D.); matsuo-n@aist.go.jp (N.M.); yuasa-s@aist.go.jp (S.Y.)

[2] Chiba Institute of Technology, 2-17-1 Tsudanuma, Narashino, Chiba 275-0016, Japan

* Correspondence: h-saitoh@aist.go.jp; Tel.: +81-29-861-5457

Received: 28 August 2017; Accepted: 20 October 2017; Published: 23 October 2017

Abstract: We investigated the effect of a thin MgO underlying layer (~3 monoatomic layers) on the growth of GaO_x tunnel barrier in Fe/GaO_x/(MgO)/Fe(001) magnetic tunnel junctions. To obtain a single-crystalline barrier, an in situ annealing was conducted with the temperature being raised up to 500 °C under an O_2 atmosphere. This annealing was performed after the deposition of the GaO_x on the Fe(001) bottom electrode with or without the MgO(001) underlying layer. Reflection high-energy electron diffraction patterns after the annealing indicated the formation of a single-crystalline layer regardless of with or without the MgO layer. Ex situ structural studies such as transmission electron microscopy revealed that the GaO_x grown on the MgO underlying layer has a cubic $MgAl_2O_4$-type spinel structure with a (001) orientation. When without MgO layer, however, a Ga-Fe-O ternary compound having the same crystal structure and orientation as the crystalline GaO_x was observed. The results indicate that the MgO underlying layer effectively prevents the Fe bottom electrode from oxidation during the annealing process. Tunneling magneto-resistance effect was observed only for the sample with the MgO underlying layer, suggesting that Ga-Fe-O layer is not an effective tunnel-barrier.

Keywords: magnetic tunnel junction; epitaxial growth; gallium oxide; tunneling magneto-resistance; semiconductor

1. Introduction

Magnetic tunnel junctions (MTJs) have been intensively studied for various applications including magnetic sensors [1–5]. In MTJs, tunneling magnetoresistance (MR) ratio is one of the most important performance indexes and defined as $(R_{AP} - R_P)/R_P$ where R_P and R_{AP} are the resistances between the two ferromagnetic (FM) electrodes with parallel and antiparallel magnetization alignments, respectively. Fabrication of epitaxial structure is the key to achieving a high MR ratio because the coherent spin-polarized tunneling in fully epitaxial MTJs yields giant MR ratios [6–8], even at room temperature (RT), as reported in MTJs with insulating tunnel-barriers such as MgO [9–11], $MgAl_2O_4$ [12], and $MgGa_2O_4$ [13].

Semiconductors (SC) have great potential as the tunnel-barrier of MTJ for a low resistance-area product [14,15] because of its rather narrow band-gap, compared with insulators. Also, fully single-crystalline FM/SC/FM structure is one of the important building blocks of a vertical-type spin field-effect-transistor having nonvolatile memory functionality [16–19]. Here, the FM layer and SC layer each respectively act as source/drain electrodes and channel layer of the FET. Note that it is impossible to realize this device by using an insulator as the channel layer. In our previous studies,

we have reported high MR ratios up to ~100% at RT in fully epitaxial Fe(001)/GaO_x(001)/MgO(001)/Fe(001) MTJs where GaO_x is a wide-gap semiconductor with a $MgAl_2O_4$-type cubic spinal structure (γ phase) [20,21]. Thanks to the coherent spin-polarized tunneling, the observed MR ratio is several times higher than those reported in MTJs consisting of polycrystalline FM electrodes with an amorphous GaO_x barrier (at most ~22% at RT) [22–24]. This is the highest value among the reported MTJs with a SC barrier at RT [14,15,22–31]. It was found in the fully epitaxial MTJs that the growth of a few monoatomic (ML; 1 ML = 0.21 nm) MgO(001) underlying layers on the Fe(001) bottom electrode are indispensable to realize a high MR ratio and that a tunneling MR (TMR) effect cannot be observed without the MgO underlying layer. Cross-sectional observations of the Fe/GaO_x/(MgO)/Fe showed sharp barrier/electrode interfaces without having the Fe layers oxidized [20,21], as expected from the observed high MR ratio. The reason for the absence of TMR effect however, is not clear since the role of the MgO layer on the growth of the GaO_x tunnel-barrier has not been clarified yet.

In this study, we performed detailed structural studies on the epitaxial MTJ structure to clarify the effects of the MgO underlying layer on the growth of the GaO_x barrier layer as well as their influence upon the TMR effect.

2. Experimental Procedures

MTJ films as shown in Figure 1 were grown by molecular beam epitaxy (MBE) in the identical type of growth chamber as mentioned in our previous study [20,21].

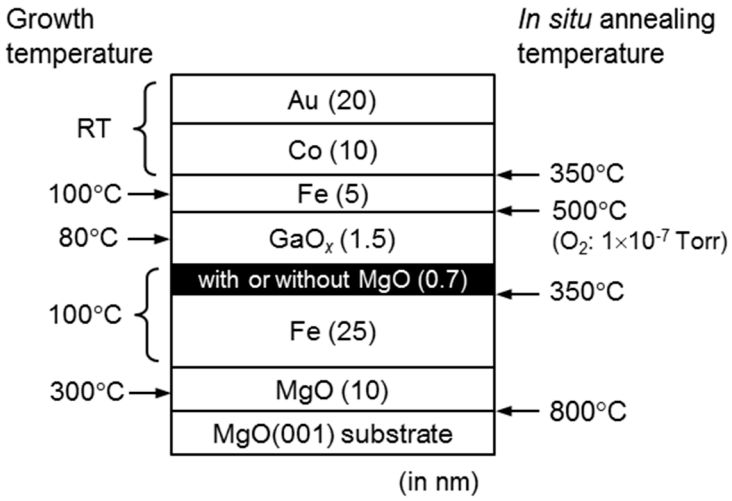

Figure 1. The structure of the magnetic tunnel junction (MTJ) stack designed for this study. Figures at both sides show growth temperatures and in situ annealing conditions.

In growing oxide layers, single-crystal Ga_2O_3 and MgO blocks were used as source materials. Prior to the growth, the MgO(001) substrate was heated at 800 °C for surface cleaning. Then, the MgO buffer layer and Fe bottom electrode are respectively grown at 300 and 100 °C, followed by an in situ annealing at 350 °C for 10 min under an ultra-high vacuum (<1 × 10^{-9} Torr) to improve surface morphology of the Fe bottom electrode. After the growth of a 0.7 nm-thick MgO underlying layer (~3 MLs), a GaO_x layer (~1.5 nm) was deposited on the Fe bottom electrode at 80 °C under an O_2 pressure of 1 × 10^{-6} Torr. Because the surface of the GaO_x layer in the as-grown state is amorphous [21], an in situ annealing for crystallizing the surface region of the GaO_x layer was carried out at temperatures up to 500 °C under an O_2 pressure of 1 × 10^{-7} Torr. After the annealing, the Fe upper electrode was grown at 100 °C and then annealed again for 10 min at 350 °C under the vacuum to improve the crystalline quality and morphology. Finally, Co-pinned and Au-cap layers were deposited at RT. The Co layer enhances the coercive force of Fe upper electrode so as to realize

the antiparallel magnetization alignment (so called pseudo-spin valve structure). For comparison, we also prepared the same structure but without the MgO underlying layer on the Fe bottom electrode.

Tunnel junctions (3 × 12 μm^2) for the magneto-transport measurements were fabricated using conventional micro-fabrication techniques [20,21]. Magneto-transport properties of the tunnel junction were measured using a conventional two probe method. The magnetic fields were applied parallel to the major axis of the junction corresponding to the easy axis of the magnetization direction of the FM electrodes.

3. Results and Discussions

Figure 2a,b show the reflection high-energy electron diffraction (RHEED) images of the GaO_x layer for the MTJ samples with or without the MgO underlying layer respectively, after the in situ annealing, with the temperature being raised up to 500 °C under the O_2 atmosphere.

(**a**) (**b**)

Figure 2. Reflection high-energy electron diffraction (RHEED) images of the GaO_x layer grown on the (**a**) MgO underling layer and (**b**) Fe bottom electrode after an *in-situ* annealing ((110) azimuth of MgO substrate).

The RHEED images of both samples showed similar streaky patterns, indicating the formation of single-crystalline layer with an atomically flat surface in both samples. Also, very similar streaky patterns appeared in the image of the Fe upper electrodes after the annealing in the vacuum. No clear difference from the RHEED observations was observed between both samples. We found however, a remarkable difference in cross-sectional transmission electron microscopy (TEM) images between both samples as given in Figure 3a,b.

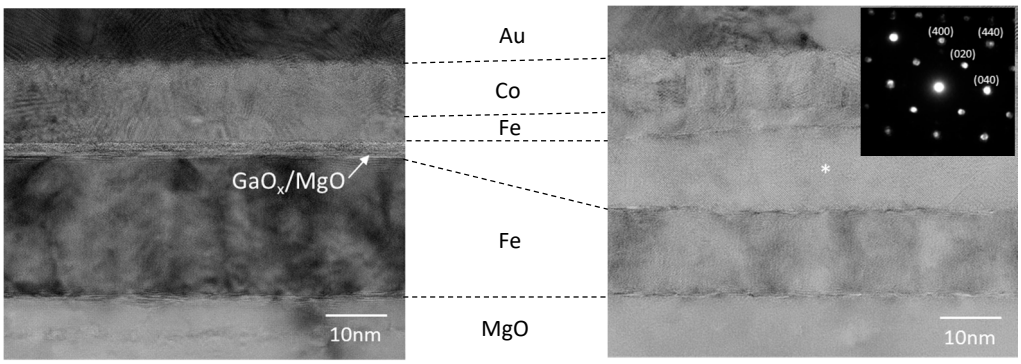

(**a**) (**b**)

Figure 3. Cross-sectional transmission electron microscope (TEM) images of the MTJ samples (**a**) with (**b**) without the MgO underlying layer ([100] azimuth of the MgO substrate). Broken lines indicate the interfaces among the layers. The inset of Figure 3b shows electron nano-beam diffraction pattern at the point indicated by an asterisk symbol.

For the sample with MgO underlying layer, a fully epitaxial Fe/GaO_x/(MgO)/Fe structure was recognized as shown in Figure 3a. Total thickness of the GaO_x/MgO layers was estimated to be about 2.2 nm which is close to the designed total thicknesses of the MgO (0.7 nm) and GaO_x (~1.5 nm)

layers. In the case without the MgO underlying layer (Figure 3b), on the other hand, a thick (~15 nm) unknown single-crystalline layer appeared between the Fe upper and bottom electrodes. Note that the thickness of the Fe bottom electrode largely decreased due to the formation of the thick unknown layer. These results imply that a part of the Fe bottom electrode was oxidized and intermixed with Ga caused by the in situ annealing at high temperature up to 500 °C under the O_2 atmosphere.

Electron nanobeam diffraction (NBD) patterns revealed that the unknown layer (the inset of Figure 3b) could be assigned as a cubic $MgAl_2O_4$-type spinel structure which is identical to that of the GaO_x tunnel-barrier. Crystal orientations of the Fe electrodes and the spinel layer were also determined as upper Fe(001)[110] ◎ spinel (001)[100] ◎ bottom Fe(001)[110] from the NBD analysis. The observed crystal orientations of the Fe electrodes and oxide (spinel) layer are identical to those of epitaxial Fe/γ-GaO_x/(MgO)/Fe MTJ [20,21]. Therefore, it is not surprising that there is no clear difference in the RHEED images between the samples with or without the MgO underlying layer.

We performed a composition analysis in the vicinity of the spinel layer by an energy-dispersive X-ray spectroscopy (EDX) as displayed in Figure 4a–c, together with the cross-sectional scanning TEM image observation (Figure 4d) as the EDX analysis.

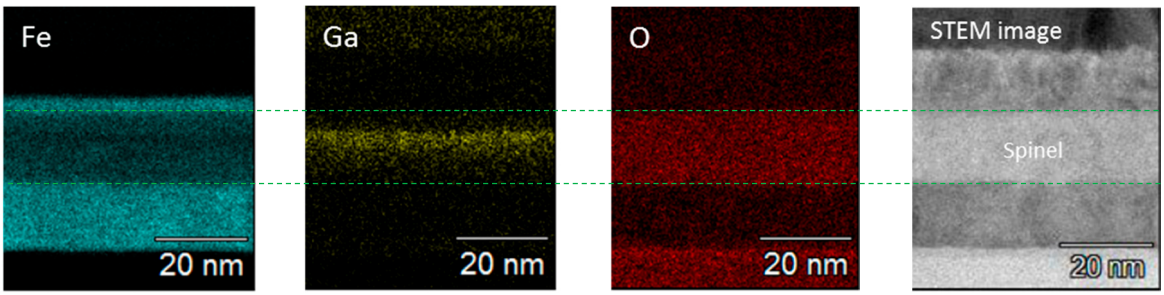

(**a**) (**b**) (**c**) (**d**)

Figure 4. Elemental mappings of (**a**) Fe, (**b**) Ga, and (**c**) O obtained from the MTJ without the MgO underlying layer using an energy-dispersive X-ray spectroscopy (EDX); (**d**) bright-field scanning TEM image of the same area. Broken lines indicate the interfaces between the spinel layer and Fe electrodes.

The spinel layer clearly consists of Fe, Ga, and O. Large amount of the distributions of Ga and Fe compositions were detected within the layer whereas O composition was also being detected with uniform distribution. This suggests that $(Fe, Ga)_2O_3$ and $(Fe, Ga)_3O_4$ are the possible materials for the observed spinel layer. It should be mentioned here that we have observed in a similar structure as the present sample with the MgO underlying layer, that there are the two distinct layers of GaO_x and MgO without being subjected to losing the thickness of the Fe bottom electrode [20]. The results indicate that a very thin (~3 MLs) MgO underlying layer effectively acts as an oxygen-preventing layer to the Fe bottom electrode during the annealing under the O_2 atmosphere.

TMR effect was only observed in sample with MgO underlying layer. The observed MR ratio was 91% at RT, which is close to the reported values in the epitaxial Fe/GaO_x/(MgO)/Fe MTJs [20,21] and several times larger than those of the MTJs with an amorphous GaO_x barrier [22–24]. For the sample without the MgO layer however, no TMR effect was observed down to 20 K. We observed a metallic behavior in temperature dependence of the junction resistances, i.e. the junction resistance decreased with decreasing temperature. Moreover, although there is a 15 nm-thick Ga-Fe-O spinel layer between the electrodes, the junction resistances were almost comparable to the parasitic resistance (~10 Ω at RT) which mainly comes from the resistance of the Fe bottom layer. The results imply that the spinel layer has poor electrical characteristics as an insulator.

4. Conclusions

We have grown epitaxial Fe/GaO_x/(MgO)/Fe(001) MTJ structure with or without the MgO underlying layer and investigated the effects of the MgO layer on the growth of GaO_x tunnel barrier

together with their influence on the TMR effect. It was demonstrated that, when the MgO layer is absent, a thick Ga-Fe-O layer having a spinel-type crystal structure was formed by conducting in situ annealing with the temperature being raised up to 500 °C under the O_2 atmosphere. As a result, no TMR effect was observed in the sample without the MgO layer. The results indicate that the MgO underlying layer effectively prevents the Fe bottom electrode from oxidation during the annealing process.

Acknowledgments: This work was supported by the ImPACT Program of the Council for Science, Technology and Innovation (Cabinet Office, Government of Japan) and Grant-in-Aid for Scientific Research on Innovative Area, "Nano Spin Conversion Science" (Grant No. 26103003).

Author Contributions: S.K.N. and H.S. conceived and designed the experiments; N.S.K., N.D. and N.M. performed the experiments; All authors contributed to discussion and analysis of the research and to the writing of the paper.

Conflicts of Interest: The authors declare no conflict of interest.

References

1. Tondra, M.; Daughton, J.M.; Wang, D.; Beech. R.S.; Fink, A.; Taylor, J.A. Picotesla field sensor design using spin-dependent tunneling devises. *J. Appl. Phys*. **1998**, *83*, 6688–6690, doi:10.1063/1.367861.
2. Freitas, P.P.; Ferreira, R.; Cardoso, S.; Cardoso, F. Magnetoresistive sensors. *J. Phys. Condens. Matter* **2007**, *19*, 165221, doi:10.1088/0953-8984/19/16/165221.
3. Lei, Z.Q.; Li, G.J.; Egelhoff, W.F.; Lai, P.T.; Pong, P.W.T. Review of noise sources in magnetic tunnel junctions Sensors. *IEEE Trans. Mag*. **2011**, *47*, 602–612, doi:10.1109/TMAG.2010.2100814.
4. Kato, D.; Oogane, M.; Fujiwara, K.; Nishikawa, T.; Naganuma, H.; Ando, Y. Fabrication of magnetic tunnel junctions with amorphous CoFeSiB ferromagnetic electrodes for magnetic field sensor devices. *Appl. Phys. Express* **2013**, *6*, 103004, doi:10.7567/APEX.6.103004.
5. Cardoso, S.; Leitao, D.C.; Gameiro, L.; Cardoso, F.; Ferreira, R.; Paz, E.; Freitas, P.P. Magnetic tunnel junction sensors with pTesla sensitivity. *Microsyst. Technol*. **2014**, *20*, 793–802, doi:10.1007/s00542-013-2035-1.
6. MacLaren, J.M.; Zhang, X.G.; Butler, W.H.; Wang, X. Layer KKR approach to Bloch-wave transmission and reflection: Application to spin-dependent tunneling. *Phys. Rev. B* **1999**, *59*, 5470–5478, doi:10.1103/PhysRevB.59.5470.
7. Mathon, J.; Umerski, A. Theory of tunneling magnetoresistance of an epitaxial Fe/MgO/Fe(001) junction. *Phys. Rev. B* **2001**, *63*, 2204031–2204034, doi:10.1103/PhysRevB.63.220403.
8. Butler, W.H.; Zhang, X.G.; Schulthess, T.C.; MacLaren, J.M. Spin-dependent tunneling conductance of Fe|MgO|Fe sandwiches. *Phys. Rev. B* **2001**, *63*, 054416, doi:10.1103/PhysRevB.63.054416.
9. Yuasa, S.; Nagahama, T.; Fukushima, A.; Suzuki, Y.; Ando K. Giant room-temperature magnetoresistance in single-crystal Fe/MgO/Fe magnetic tunnel junctions. *Nat. Mater.* **2004**, *3*, 868–871, doi:10.1038/nmat1257.
10. Parkin, S.S.P.; Kaiser, C.; Panchula, A.; Rice, P.M.; Hughes, B.; Samant, M.; Yang, S.H. Giant tunnelling magnetoresistance at room temperature with MgO (100) tunnel barriers. *Nat. Mater.* **2004**, *3*, 862–867, doi:10.1038/nmat1256.
11. Djayaprawira, D.D.; Tsunekawa, K.; Nagai, M.; Maehara. H.; Yamagata, S.; Watanabe, N. 230% room-temperature magnetoresistance in CoFeB/MgO/CoFeB magnetic tunnel junctions. *Appl. Phys. Lett.* **2005**, *86*, 092502, doi:10.1063/1.1871344.
12. Sukegawa, H.; Xiu, H.; Ohkubo, T.; Furubayashi, T.; Niizeki, T.; Wang, W.; Kasai, S.; Mitani, S.; Inomata, K.; Hono, K. Tunnel magnetoresistance with improved bias voltage dependence in lattice-matched Fe/spinel $MgAl_2O_4$/Fe(001) junctions. *Appl. Phys. Lett.* **2010**, *96*, 212505, doi:10.1063/1.3441409.
13. Sukegawa, H.; Kato, Y.; Belmoubari k, M.; Cheng, P.H.; Daibou, T.; Shimomura, N.; Kamiguch, Y.; Ito, J.; Yoda, H.; Ohkubo, T.; Mitani, S.; Hono, K. $MgGa_2O_4$ spinel barrier for magnetic tunnel junctions: Coherent tunneling and low barrier height. *Appl. Phys. Lett*. **2017**, *110*, 122404, doi:10.1063/1.4977946.
14. Uehara, Y.; Furuya, A.; Sunaga, K.; Miyajima, T.; Kanai, H. Magnetic tunnel junctions with low resistance-area product of 0.5 $\Omega\mu m^2$. *J. Magn. Soc. Jpn*. **2010**, *34*, 311–315, doi:10.3379/msjmag.1003R027.
15. Kasai, S.; Takahashi, Y.K.; Cheng, P.H.; Ikhtiar; Ohkubo, T.; Kondou, K.; Otani, Y.; Mitani, S.; Hono, K. Large magnetoresistance in Heusler-alloy-based epitaxial magnetic junctions with semiconducting $Cu(In_{0.8}Ga_{0.2})Se_2$ spacer. *Appl. Phys. Lett*. **2016**, *109*, 032409, doi:10.1063/1.4959144.

16. Kanai, T.; Asahara, H.; Ohya, S.; Tanaka, M. Spin-dependent transport properties of a GaMnAs-based vertical spin metal-oxide-semiconductor field-effect transistor structure. *Appl. Phys. Lett*. **2015**, *107*, 242401, doi:10.1063/1.4937437.
17. Yamada, S.; Tanikawa, K.; Miyao, M.; Hamaya, K. Atomically controlled epitaxial growth of single-crystalline germanium films on a metallic silicide. *Cryst. Growth Des*. **2012**, *12*, 4703–4707, doi:10.1021/cg300791w.
18. Jenichen, B.; Herfort, J.; Jahn, U.; Trampert, A.; Riechert, H. Epitaxial Fe_3Si/Ge/Fe_3Si thin film multilayers grown on GaAs(001). *Thin Solid Films* **2014**, *556*, 120–124, doi:10.1016/j.tsf.2014.01.022.
19. Kawano, M.; Ikawa, M.; Santo, S.; Sakai, S.; Sato, H,; Yamada, S.; Hamaya, K. Electrical detection of spin accumulation and relaxation in *p*-type germanium. *Phys. Rev. Mater*. **2017**, *1*, 034604, doi:10.1103/PhysRevMaterials.1.034604.
20. Matsuo, N.; Doko, N.; Takada, T.; Saito, H.; Yuasa, S. High magnetoresistance in fully epitaxial magnetic tunnel junctions with a semiconducting GaO_x tunnel barrier. *Phys. Rev. Appl.* **2016**, *6*, 034011, doi:10.1103/PhysRevApplied.6.034011.
21. Narayananellore, S.K.; Doko, N.; Matsuo, N.; Saito, H.; Yuasa, S. Investigation on the formation process of single-crystalline GaO_x barrier in Fe/GaO_x/MgO/Fe magnetic tunnel junctions. *J. Phys. D Appl. Phys.* **2017**, *50*, 435001, doi:10.1088/1361-6463/aa861b.
22. Li, Z.; de Groot C.; Moodera, J.S. Gallium oxide as an insulating barrier for spin-dependent tunneling junctions. *Appl. Phys. Lett*. **2000**, *77*, 3630–3632, doi:10.1063/1.1329169.
23. Parkin, S.S.P. Magnetic Tunnel Junction Device with Improved Insulating Tunnel Barrier. U.S. Patent No. 6359289, 19 March 2002.
24. Watanabe, S.; Saito, H.; Mineno, Y.; Yuasa, S.; Ando, K. Origin of very low effective barrier height in magnetic tunnel junctions with a semiconductor GaO_x tunnel barrier. *Jpn. J. Appl. Phys*. **2011**, *50*, 113002, doi:10.1143/JJAP.50.113002.
25. Rottländer, P.; Hehn, M.; Lenoble, O.; Schuhi, A. Tantalum oxide as an alternative low height tunnel barrier in magnetic junctions. *Appl. Phys. Lett*. **2001**, *78*, 3274–3276, doi:10.1063/1.1374223.
26. Guth, M.; Dinia, A.; Schmerber, G.; van den Berg, H.A.M. Tunnel magnetoresistance in magnetic tunnel junctions with a ZnS barrier. *Appl. Phys. Lett*. **2001**, 78 3487–3489, doi:10.1063/1.1372206.
27. Gustavsson, F.; George, J.M.; Etgens, V.H.; Eddrief, M. Structural and transport properties of epitaxial Fe/ZnSe/FeCo magnetic tunnel Junctions. *Phys. Rev. B* **2001**, *64*, 184422, doi:10.1103/PhysRevB.64.184422.
28. Kreuzer, S.; Moser, J.; Wegscheider, W.; Weiss, D.; Bichler, M.; Schuh, D. Spin polarized tunneling through single-crystal GaAs(001) barriers. *Appl. Phys. Lett*. **2002**, *80*, 4582–4584, doi:10.1063/1.1486044.
29. Jiang, X.; Panchula, A.F.; Parkin, S.S.P. Magnetic tunnel junctions with ZnSe barriers. *Appl. Phys. Lett*. **2003**, *83*, 5244–5246, doi:10.1063/1.1630160.
30. Androulakis, J.; Gardelis, S.; Giapintzakis, J.; Gagaoudakis, E.; Kiriakidis, G. Indium oxide as a possible tunnel barrier in spintronic devices. *Thin Solid Films* **2005**, *471*, 293–297, doi:10.1016/j.tsf.2004.06.162.
31. Kobayashi, K.; Akimoto, H. TMR film and head technology. *FUJITSU Sci. Tech. J*. **2006**, *42*, 139–148.